Compression after impact test (CAI) on NOMEX™ honeycomb sandwich panels with thin aluminum skins

A. Gilioli, C. Sbarufatti, A. Manes *, M. Giglio

Politecnico di Milano, Dipartimento di Meccanica, Via la Masa 1, 20156, Milano, Italy

Received 28 November 2013 Received in revised form 4
June 2014 Accepted 10 July 2014
Available online 25 July 2014

1. Outlook

The use of optimized lightweight structures in the transportation field and especially in aerospace components is nowadays very common. This kind of components can lead to a significant reduction of the overall weight of vehicles, aircrafts, trains, etc., keeping a relevant reliability and a good performance as well. Good examples of such components are sandwich panels that exhibit in plane strength and significant flexural stiffness, thus representing an optimal solution respect to monolithic configuration.

In the present research the work is focused on sandwich panels having thin (1 mm or 1.5 mm) aluminum skins and a Nomex™ honeycomb core. Real application of these structures can be found in helicopter fuselages. A contingent environment can expose such sandwich panels to a wide range of possible damage scenarios and, among them, one of the most severe regards low velocity impacts. The low velocity impact loading condition is also one of the reasons for the choice of adopting aluminum for skins. Aluminum alloy is a weight efficient ductile material able to absorb energy by localized deformation; according to [1] low velocity impacts on sandwich panels can lead to a 50% decrease on their structural strength. Hence it is clear why such events are so important to study. The present work can be considered as an evolution of [2]. In that paper low velocity impacts have been experimentally and numerically investigated: an experimental campaign, using a drop tower apparatus, was carried out to study the low velocity impact behavior of such sandwich panels. In the present research, starting from the experimental data collected in [2], identical sandwich panels have been investigated with the main goal to establish quantitatively their loss of mechanical strength after impact. Compression after impact (CAI) experimental campaign, inspired to the C 364/C 364M – 07 standard [3], has been therefore carried out. Various factors have been considered to establish their influence over CAI strength, in particular impact occurrence, aluminum skin thickness and impact energy. Experimental data obtained are herein reported together with a statistical analyzes and a discussion of the results obtained.

From an historical point of view, the importance of the evaluation of the structural integrity of components having some defects inside became important from the 70s and in particular in the 80s with the spread of composite structures in the aerospace field. A typical example of possible unwanted defect involved low-velocity impacts. Test methods were developed to study these

* Corresponding author. Tel.: +39 02 2399 8630; fax: +39 02 2399 8282.
E-mail address: andrea.manes@polimi.it (A. Manes).

scenarios consisting of a specific impact event followed by an in-plane compression loading to failure. Two methods emerged as the most prominent: one from the NASA-Langley Research Center [4] and another developed subsequently by the Boeing Corporation [5]. The Boeing CAI method was adopted, essentially unchanged, as ASTM Standards D7136 [6] for the impact event and as D7137 [7] for the compression after impact portion of the test and its version of the CAI fixture is the most spread at present. The above-mentioned citations refer to laminate composite panels, but more related papers with the topic of the research can be found among the work of FAA and especially in [8,9] concerning sandwich structures.

The literature mainly contains papers concerning CAI tests on full composite sandwich panels where skins are manufactured in composite material too. As previously mentioned, although metallic materials do not exhibit high "tailoring" design capability, their ductility is an interesting property in a balanced design process where impact loadings are a possible and an actual risk. The research carried out in [10] regards a CAI test on similar sandwich panels with thin brass skins and a Nomex™ honeycomb core. An image correlation technique was applied to track the changes of the damage shape as a function of the applied load. Results show how an initial almost circular damage tends to become elliptical with an increasing load. The authors further underlined how the indentation is a localized phenomenon, thus the results are unaffected by the boundary conditions. In [11] the authors studied a sandwich panel having a Nomex™ honeycomb core but a woven fabric carbon epoxy face-sheet. They also developed a semi empirical model able to describe the CAI test. In [12] the authors studied experimentally the impact and the CAI test on sandwich panels having a foam core and Kevlar skins. A similar experimental set was used in [13] where the authors studied sandwich structures with a PVC foam core and woven carbon/epoxy face sheets. In [14] the authors experimentally studied sandwich panels with a foam core demonstrating that the CAI strength decreases with an increasing impact damage size. The authors of [15] built a curve relating the CAI strength to the impact energy for the honeycomb sandwich panels with FRP (fiber reinforced polymer) skins. Instead of the CAI test, to assess the residual strength of the impacted panels, a 4 points bending test was exploited in [16] to evaluate panels having aramid paper fold-cores and carbon-fiber reinforced plastic (CFRP) skins. Impact on sandwich panels with a Nomex™ honeycomb core and aluminum skins was studied in [17] and by the same authors of the present research in [18] but in both cases the impact velocity is much higher than in the current research (160–800 m/s vs. 7 m/s).

The current paper is part of a wider research project developed by the same authors in [2,19,20]. The final aim of the research is to characterize the material properties and the behavior of sandwich panels with Al2024 aluminum skins and a Nomex™ honeycomb core, with the goal to assess their mechanical properties under contingent and extreme loads and to eventually develop a real-time structural health monitoring (SHM) system able to identify impact occurrences as well as the state and evolution of the item when damaged. Additional information regarding the use of sensors to describe low velocity impacts on sandwich panels can be found in [21], while [22] is another valid example of the application for Carbon Fiber Reinforced Plastic plates. As a matter of fact, by adding an appropriate number of sensors to the panels, it is possible to recognize the occurrence of low velocity impacts, their impact location and their energy, the latter being the biggest signal processing challenge. Once these variables have been estimated through the sensor network, only one important information is missing: the decrement of the performance for the considered structure (structural integrity reduction) resulting from the identified impact. Obtaining this information is a crucial step of the research, which is presented in the current paper.

The paper is structured as follows. The experimental activity is presented in Section 2, specifically concerning the drop test for low velocity impacts (Section 2.1), the acquisition of the damage shape (Section 2.2) and the compression test on intact and impacted sandwich panels (Section 2.3). A sensitivity analysis is carried out in Section 3, based on the experimental data. A graphical evaluation of the influence of different factors on the compressive strength is firstly performed in Section 3.1, followed by a statistical assessment of each factor influence based on the *analysis of variance* theory (Section 3.2). A conclusive section is finally provided.

2. Experimental activity

Tested sandwich panels (Fig. 1c) are made with a Nomex™ honeycomb core and thin Al2024-T3 aluminum alloy skins. The honeycomb core is made by Nomex™, whose trade name is A10, and is manufactured by Hexcel Composite. It consists of DuPont's Nomex™ aramid-fiber paper, dipped in a heat-resistant phenolic resin. Its characteristics are high strength and toughness in a small cell size with low volumic mass (32 kg/m^3). A thermosetting adhesive is used to bond these sheets at the nodes and, after expanding to the hexagonal configuration, the block is dipped in phenolic resin. In particular, the tested honeycomb core has a trade code: A10-32-5. According to the datasheet of the manufacturer [23], the code refers to the geometrical and mechanical characteristics of the honeycomb core, as described in Table 1. The core is linked to upper and lower metallic plates using a modified epoxy film adhesive Redux™ 312. The metallic skins of the panels are made by an Al2024-T3 aluminum alloy. The characterization of the skin material constitutive law (based on the Johnson–Cook law) has been previously presented by the authors in [2], including also the calibration of a proper ductile damage criterion. A summary of the material properties for the panel skins is reported for completeness in Table 2.

Two different specimen geometries have been tested, both having the same global thickness (22 mm) but a different skins/core thickness ratio, as indicated in Table 3.

The experimental activity consists of three different steps for each panel specimen:

- Low velocity impact using a drop tower setup.
- Acquisition of the damage shape using coordinate measurement tool.
- Compression after impact (CAI) test.

The data regarding the first two points is taken from previous research by the same authors in [2] and is briefly summarized in Section 2.1. A description of the CAI tests is presented in Section 2.2, where a report on the experimental data is also provided.

2.1. Low velocity impact and damage shape acquisition

The drop tests for low velocity impact consist in a guided mass falling through a tube and eventually impacting a 400 × 400 mm sandwich panel, properly grounded by means of two rigid frames (Fig. 1a and b). The free fall height, as well as the weight of the impactor, are modifiable to allow testing in a large energy range (15–241 J). Each panel has been submitted to a single impact.

The impactor has a spherical nose shape with a diameter of 25.4 mm. In order to evaluate the real impact energy, a laser device has been used to acquire the impactor velocity at the exit of the tube. Hence it has been possible to calculate the kinetic energy of the impactor very close to the target panel, taking into account all the possible dissipation issues. Once the panels have been tested, the damage shapes are acquired using a Zeiss Prismo 5

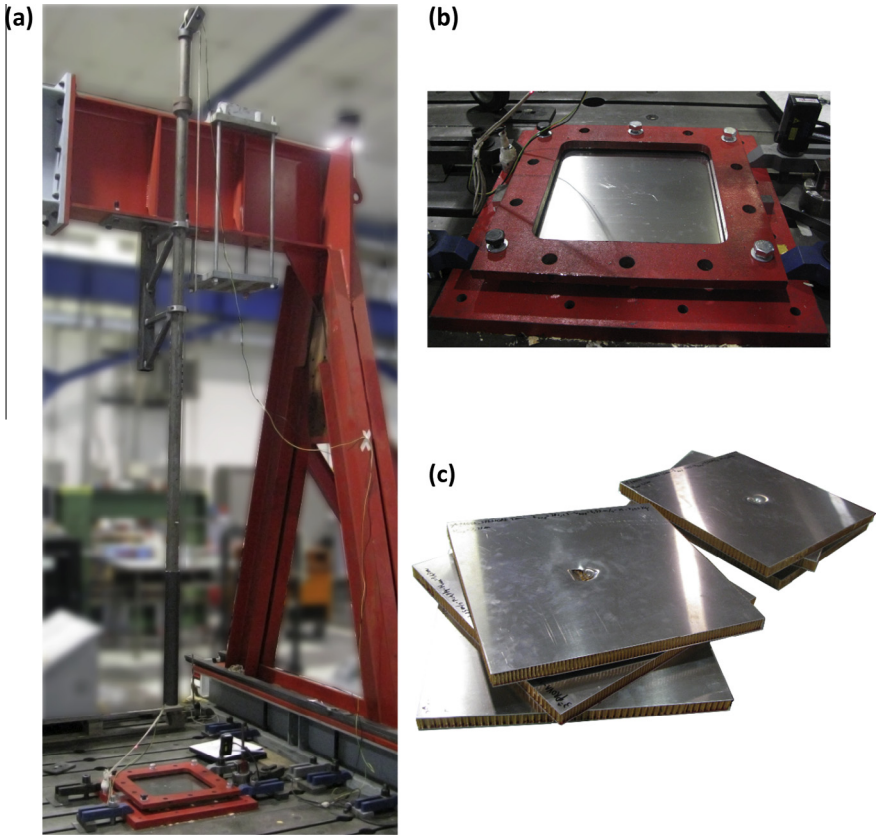

Fig. 1. (a) Test rig for the drop test; (b) focus on the rigid frame for panel grounding during the impact test and (c) examples of sandwich panel specimens after impact tests.

Table 1
Honeycomb designation and nomenclature.

Code: A10-32-5	Meaning
A10	Designates honeycomb type
5	Cell size (mm)
32	Nominal volumic mass (kg/m^3)

Table 2
Material calibration of the constitutive law (Johnson–Cook law) for the aluminum alloy Al2024-T3.

Constitutive law (Johnson–Cook law) $\sigma = A + B\varepsilon^n$	
A	335.1 MPa
B	511.6 MPa
n	0.4524
E (Young modulus)	68,710 MPa
ν (Poisson ratio)	0.33

HTG coordinate measuring apparatus. According to ISO 10360-2, the measures have been carried out adopting an accuracy of 1.4 µm + L/330 [µm/mm] (18–22 °C). The profile of the impacted skin has been firstly measured along two orthogonal directions, parallel to the panel edges, covering a square area of ±120 mm around the impact point. Also the two diagonals of this square have been acquired (Fig. 2). Measurement data have been acquired every 0.1 mm. The origin of the coordinate system has been put in the lowest point of the scanned surface, thus the origin of the measurement axis is the point with the maximum depth. Due to the localized nature of the damage, obtained by adopting such acquisition setup parameters, it has been possible to cover and analyze a region that is large enough to include the most relevant phenomena. The use of a finer discretization grid, or the evaluation of a larger area, does not lead to a relevant increment of the quality results but only to a possible increment of the noise inside the measurements and to the acquisition of irrelevant data (study of a barely undamaged area). Two parameters have been extracted from the damage profile, as indicated in Fig. 3a. First, the Maximum Penetration Depth (MPD) is a measure of the maximum depth of the damage induced by the impact. The impact energy range has been purposely selected to avoid aluminum skin failure, so the evaluated panels do not have ruptured skins but only plastically deformed skins. Second, the Opening Width (OW) has been calculated as the width of the plastic zone, evaluated crossing the damage profile with a horizontal threshold line lying at a 0.1 mm distance from the undamaged reference plane. The choice of a threshold at exactly 0.1 mm is arbitrary but according with the experience of the authors, 0.1 mm is a reasonable value to guarantee significance to the measures. The adoption of a threshold horizontal value avoids some possible discrepancies due to the experimental measurement procedure.

2.2. CAI/edgewise compressive test

Compression after impact (CAI) tests have been carried out on damaged and undamaged specimens and adopting a procedure inspired by the international standards [3]. The term compression after impact tests refers to panels which have already been impacted so the tests for undamaged panels are more correctly defined as edgewise compression tests. A specific fixture system inspired to [3] has been developed (Fig. 4) and even the size of the specimen (137.5 × 137.5 mm) has been chosen following the standard. This dimension is large enough to fully include the impact damage area. According with the definition of [17], the

Table 3
Size description of the two tested panel configurations. Both configurations have the same overall thickness (22 mm) but different ratio between skin and core.

	Skin thickness (mm)	Core thickness (mm)	Overall thickness (mm)
Configuration 1	1	20	22
Configuration 2	1.5	19	22

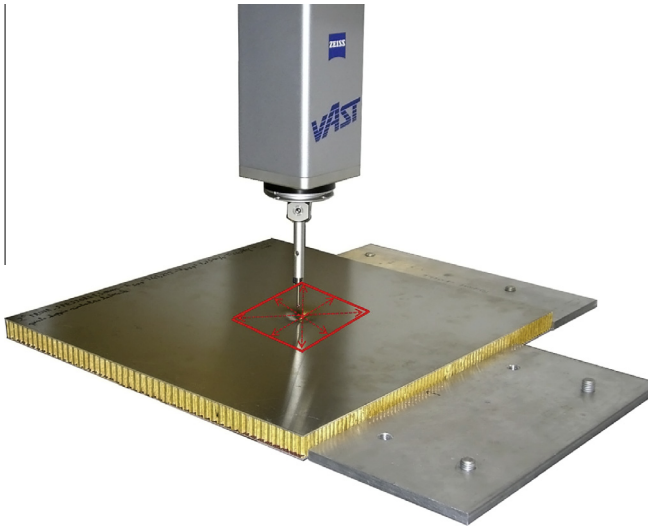

Fig. 2. Coordinate measurement tool adopted to acquire the panel damage profile with the indication of the profile measured paths: according with the red line square, profile has been acquired along the two orthogonal directions starting from the center and along the two square diagonals. (For interpretation of the references to colour in this figure legend, the reader is referred to the web version of this article.)

CAI test have been always performed keeping the honeycomb L direction always parallel with the compressive load. Impacted specimens used for the drop test (Section 2.1) have been cut to the required dimension. The CAI tests have been done adopting a MTS Alliance testing machine. The load has been acquired using a 100 kN-load cell and displacement has been acquired as the crosshead displacement. A spherical joint located between the fixture system and the upper machine head guaranteed the self-alignment of the load. Fig. 5 shows the experimental failure of an intact specimen where is clear the global buckling of the aluminum skins. The two horizontal dashed black lines reported in the figure highlights the residual deformation of the panel after testing. The permanent damage of the core is evident along two oblique lines starting from the center of the upper skin. Indeed, the hexagonal structure of the core cannot deform as imposed by the buckling shape of the skin unless there is a localized collapse of the cells as well.

Compressive force vs. crosshead displacement curves have been stored, as shown in Fig. 3b., and one relevant parameter has been extracted, namely the compression strength (either the CAI or the edgewise compression strength depending on the selected specimen, damaged or undamaged), corresponding to the peak of the curve, as indicated in Fig. 3b.

The entire test campaign is schematized in Table 4. A total number of 30 compression tests have been performed on 30 sandwich panels. In particular, 14 compression tests have been carried out on healthy panels, while 16 CAI tests have been executed on impacted specimens with different levels of impact damage. In both cases, two levels of aluminum skin thickness have been considered, corresponding to the configurations reported in Table 3, thus allowing the quantification of any possible benefits induced by a 50% increase of the skin thickness, in terms of the CAI strength. Focusing on the impacted specimens, different impact energies have been tested, aiming to estimate the effect of the impact energy (thus the effect of the plastic damage extent, the opening width, OW, and the maximum penetration depth, MPD) on the specimen CAI strength. The results have been evaluated in terms of compression strength (edgewise strength or CAI strength for intact and impacted specimens respectively). Additionally, the maximum depth and the opening width of the induced damages have been reported in Table 4 for the impacted specimens only.

Data obtained during the edgewise compression and the CAI tests for intact and damaged sandwich panels have been reported in Fig. 6, in terms of force vs. crosshead displacement relation. In order to reduce the curve dispersion due to clearance, gap and contact effects, which are usual at the beginning of compression tests, the curves are moved along the horizontal axis so that the zero-displacement always corresponds to a 5 kN applied load. This allows removing most of the non-linear portion of each curve, nevertheless without affecting the measure of CAI strength. In particular, Fig. 6a and b report the curves obtained with a 1 mm skin thickness, while Fig. 6c and d refer to the 1.5 mm skin thickness configuration. Furthermore, Fig. 6a and c are related to seven intact specimens subjected to a compressive load. Seven compression tests have thus been provided for each thickness configuration. Fig. 6b and d refer to the impacted specimens and each curve correlates with a different specimen, with a different associated damage, connected to different impact energy. The peak for each curve is the index of the compression strength and is reported in the right end column of Table 4. The impact has an obvious effect on the compression resistance of the specimens, as the CAI strength is generally lower than the edgewise compression strength. Nevertheless, the results are affected by a large dispersion, especially for pristine specimens, and proper statistical methods are necessary to form more confident conclusions on the parameters influencing the CAI strength, such as the panel skin thickness and the impact energy.

2.3. Analysis of compression curve dispersion

Before entering into the details of the statistical sensitivity analysis of CAI strength, which is reported in the next chapter, in this paragraph the attention is addressed toward the compression curves shown in Fig. 6. In particular, the dispersion of force vs. displacement curves is analyzed. The uncertainty related to edgewise compression tests (or CAI tests) is significant and it could be related to many different factors, such as geometrical tolerances of the specimens[1], assembly tolerances of the test rig and tolerances of material properties, which cannot be completely avoided. In order to summarize and compare the curves relative to impacted and non-impacted specimens having different skin thicknesses (correspondent to different sub-plots in Fig. 6), two parameters have been considered:

(i) The *deformation energy*, calculated as

$$U = \int_0^{\hat{s}} F(s)ds \tag{1}$$

[1] For the sake of completeness, tolerances of the global panel thickness (aluminum skin plus honeycomb core) have been statistically quantified as an average value of 21.98 mm and 0.106 mm standard deviation. Panel side dimension has an average value of 136.93 mm and a standard deviation of 0.615 mm. The available specimens have been measured with a caliper.

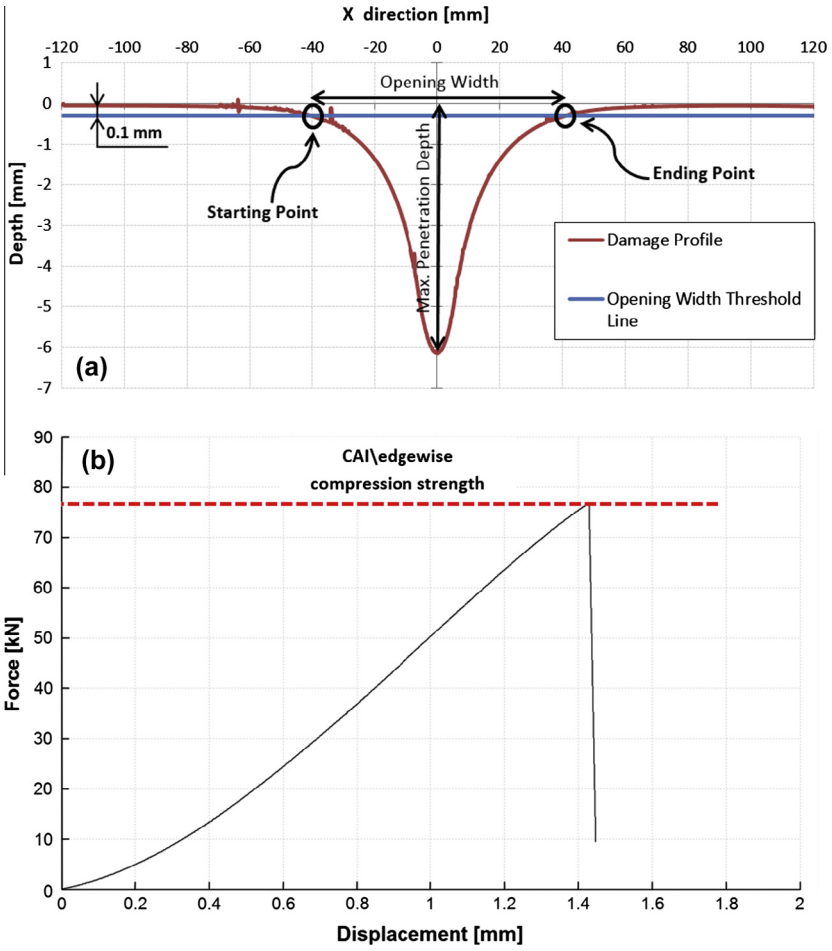

Fig. 3. Quantitative variables describing the entity of the damage shape and the panel strength (a) maximum penetration depth and opening width extraction from the damage profile and (b) CAI/edgewise compression strength extraction from the force vs. displacement curve.

where $F(s)$ is the force (dependent on displacement s) applied through the movement of the machine crosshead and $\hat{s}$ is the limit displacement for the evaluation of the deformation energy U. In particular, a limit displacement $\hat{s} = 0.4mm$ has been considered for each case reported in Fig. 6, to guarantee sufficient distance from the buckling point.

(ii) The *average stiffness*, calculated as

$$K = \frac{\int_{\hat{s}_1}^{\hat{s}_2} \frac{\partial F(s)}{\partial s} ds}{\hat{s}_2 - \hat{s}_1} \tag{2}$$

This represents an average stiffness, due to the non-linear behavior measured during experiments. Different integral boundaries $[\hat{s}_1, \hat{s}_2]$ have been considered for each case reported in Fig. 6 in order to focus on the most linear part of each curve, thus limiting the amount of non-linearity involved in the calculation of the parameter.

The two parameters have been calculated for each curve reported in Fig. 6 and their mean and their standard deviation (indicated as μ_U, σ_U for the deformation energy and as μ_K, σ_K for the average stiffness) have been reported in Table 5. Reported values refer to each considered configuration, namely:

- Intact specimens with 1 mm aluminum skin.
- Impacted specimens with 1 mm aluminum skin.
- Intact specimens with 1.5 mm aluminum skin.
- Impacted specimens with 1.5 mm aluminum skin.

It is firstly important to verify that both the mean values of the energy and the average stiffness increase if a thicker aluminum skin is considered. This check allows evaluating the reliability of the experimental data, nonetheless highlighting their variability. According with Table 5, this trend is verified for both intact and impacted specimens. Focussing on pristine specimens, a 43% increase of average stiffness was measured, due to a 50% increase of aluminum skin thickness. When impacted specimens are considered, this effect reduces to 13%. Furthermore, comparing impact/intact configurations, a reduced influence on the mean values of the energy parameter has been found in the analysis regarding the first portion of force–displacement curves (up to 0.6 mm limit displacement). Concerning the average stiffness, impact condition induces 11% and 30% parameter reduction for the 1 mm and 1.5 mm skin thickness specimens respectively.

Referring to the values of standard deviation reported in Table 5, no significant variation is found in both parameters (U and K) comparing the two configurations with 1 mm and 1.5 mm skin thickness respectively.

Comments arise whilst comparing intact and impacted specimens. As a matter of fact, a noticeable decrease of the variance is found on the impacted specimens compared with the intact ones, as it can be immediately perceived also referring to Fig. 6. Independently from the considered skin thickness, the occurrence of an impact damage (without skin failure) moderately modifies the average stiffness and the absorbed energy, while it strongly

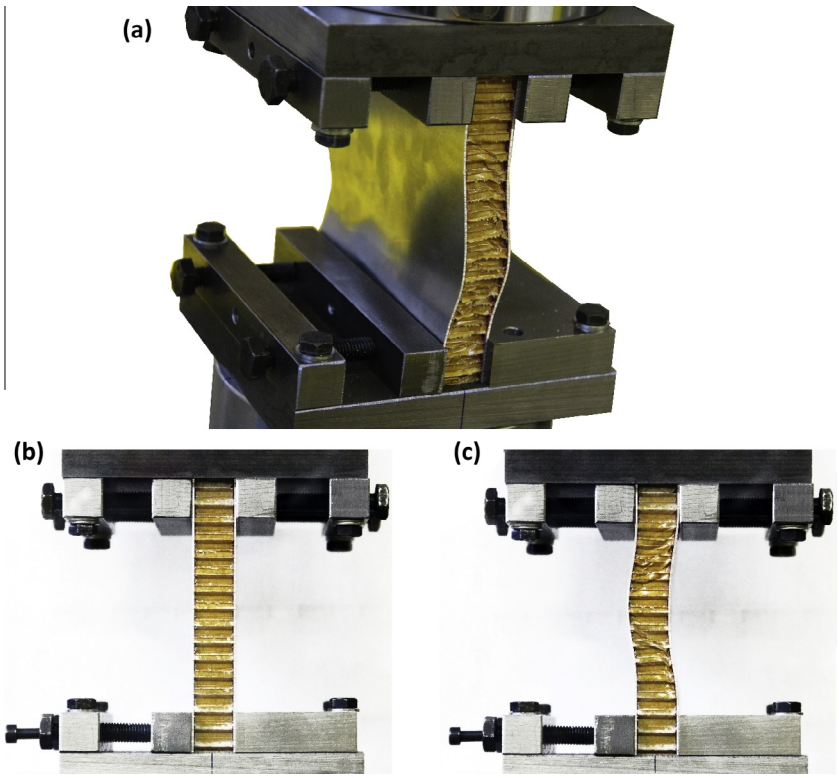

Fig. 4. (a) Prospective view of a sandwich panel specimen and the gripping system during a compression test, (b) orthogonal view of an uncompressed panel and (c) orthogonal view of a compressed panel.

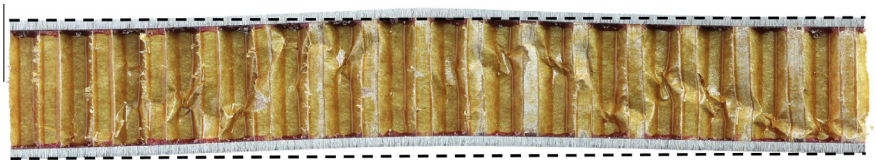

Fig. 5. An intact specimen after the CAI test. The two horizontal dashed black lines highlight the permanent deflection.

reduces the variability of the force–displacement curve, and consequently of the considered parameters. Obviously, these comments are valid before the occurrence of buckling, as can be distinguished in Figs. 6b and d.

An explanation for this behavior can be drawn considering the marginal, nevertheless effective, capability of the sandwich structure to prevent buckling. If a compressive load is applied to the structure, this will be redistributed among the aluminum skins and the honeycomb core. As a matter of fact, the hexagonal section of the honeycomb cell provides non-negligible resistance to rotations associated to the deformed final buckling shape. When the skins change their shape because of buckling (even in the case of elastic buckling) the honeycomb core has to deform permanently. Hexagonal cells cannot assume the deformed shape imposed by the aluminum skin without avoiding the buckling collapse of the Nomex core. Consequently, also the core has to buckle to permit the buckling of the skins, thus requiring a non-negligible load. Additionally, due to manufacturing tolerances, the honeycomb pattern is far from being a perfect repetition of the same elementary cell. This factor can provoke different preferential load transfer paths (and failure paths) each time a new specimen is loaded and thus this not homogeneous behavior is responsible for the dispersion of the experimental curves relative to intact specimens. On the other hand, the presence of an impact damage will sensibly modify the pattern-like structure of the honeycomb, which largely loses its buckling resistance capability. The buckling initiation point becomes much more deterministic and the aluminum skins carry the majority of the load. This will sensibly reduce the uncertainty on the force–displacement curves during CAI tests because the buckling resistance is mainly provided by the skins whose properties are much more homogeneous than for the honeycomb.

It is finally important to consider that impact damage sensibly reduces CAI strength too, as it is shown in Fig. 6 and quantified in the following sections.

3. Sensitivity analysis

As shown in Table 4, the experimental test campaign presented above takes many parameters into account. The aim of the present section is to investigate to which extent the CAI strength (or, more generally, the compression strength) is influenced by some factors: impact condition (damaged – undamaged), aluminum skin thickness and impact energy. This is particularly useful to understand which design parameter is worth modifying to improve an optimal operational condition, as well as to appreciate which are the most important factors to be monitored to guarantee the safe operation of the structure.

A preliminary investigation of the compression strength depending on the various factors is presented in Section 3.1, mainly in the form of the main effect plots. The statistical

Table 4
Summary of the entire experimental CAI/edgewise compression test programme. Each test is described in terms of impact energy and the results concerning its damage profile (OW, MPD) and its edgewise compression load are reported.

Test ID	Impact	Thickness (mm)	Impact energy (J)	MPD (mm)	OW (mm)	CAI strength[a] (kN)
1	0	1		n.a.		55.5
2	0	1				36.1
3	0	1				29.4
4	0	1				76.8
5	0	1				48.1
6	0	1				36.8
7	0	1				37.5
8	0	1.5		n.a.		80.1
9	0	1.5				84.1
10	0	1.5				52.8
11	0	1.5				81.4
12	0	1.5				78.8
13	0	1.5				47.9
14	0	1.5				62.0
15	1	1	16.3	3	71.3	38.7
16	1	1	31.6	3.9	84.6	30.9
17	1	1	59.9	5.5	86.1	19.9
18	1	1	78.7	6.7	105.6	24.2
19	1	1	112.7	7.6	113.6	20.7
20	1	1	141.6	9	105.9	18.3
21	1	1	173.3	9.5	116.4	25.0
22	1	1.5	15.3	2.2	63.7	44.6
23	1	1.5	59.6	4.3	90.6	29.6
24	1	1.5	83.9	5.3	123.1	29.7
25	1	1.5	96.9	6.1	110.4	24.2
26	1	1.5	126.3	6.8	133.7	33.3
27	1	1.5	141.6	7.7	218.0[b]	22.5
28	1	1.5	187.1	8.2	129.9	24.2
29	1	1.5	217.1	9.3	135.6	21.3
30	1	1.5	241.7	10.1	175.8	20.3

[a] In rigorous terms the CAI (compression after impact) strength should refer only to impacted specimens. The results for impacted and undamaged specimens have been included for simplicity in the same column. Regarding the impact column, 0 refers to undamaged specimen, 1 refers to damaged specimen.
[b] This value was considered as an outlier and has thus not been included in the subsequent analysis.

methodology of the *analysis of variance* (ANOVA) is adopted in Section 3.2 to statistically assess the influence of the considered factors.

3.1. Graphical evaluation of factors' influence on the compressive strength

The first question to be addressed is whether the presence of any impact damage has an effect on the sandwich panel performances in terms of compression strength. It is reasonable to predict that the presence of an impact damage will facilitate buckling instability, which is indeed well reflected in the data reported in Fig. 7. All the panel specimens presented in Table 4 have been divided into two categories, namely impacted and non-impacted. The experimental impact energy range has been selected to guarantee the production of a plastic damage on the aluminum skin and this grouping corresponds to the damage – undamaged classification. Although the compression strength appears to be widespread, especially for the intact panel configuration, a clear reduction of the CAI strength is apparent when looking at the calculated average trend.

The second factor to be investigated is the sandwich panel skin thickness with the aim to understand its effects on the compression strength. In particular, the question to be addressed is whether it is worth or not (from the point of view of buckling resistance) to increase the aluminum skin dimension, inducing an inevitable increase of the structural weight. An increment of the skin thickness from 1 mm to 1.5 mm leads to a 44% increment of the overall panel weight. In practice, the global panel thickness is kept constant (22 mm), thus the increase of the skin thickness is associated to an equivalent reduction of the core thickness. The entire experimental database available is considered in Fig. 8a, where impacted and non-impacted specimens have been included. The intensification of the compression strength due to a 50% increase of skin thickness (from 1 mm to 1.5 mm) can be evaluated referring to the average trend and corresponds to about 36%. Nevertheless, the experimental data dispersion is very high, corresponding to nearly 500% with respect to the shift of the average trend, which makes difficult to draw any conclusion about the influence of the selected factor. The same is valid when looking at Fig. 8b and c, where the impacted and the intact specimens have been separately included. If the impacted specimens are considered (Fig. 8b), the change in skin thickness provokes a 9% increase in CAI resistance, while this effect raises to 52% if only the intact specimens are taken into account (Fig. 8c). It is clear that the skin thickness has a higher contribution to compressive strength when the panel is undamaged (Fig. 8c), while the factor becomes less evident after the impact damage has been induced (Fig. 8b).

The third and last investigated factor is the impact energy. Only the impacted specimens are considered at this level. It is presumable that the higher the impact energy is, the worse the damage condition will be. As a matter of fact, this is reflected in the experimental results reported in Figs. 9a and b, where the maximum depth penetration and the opening width of the impact damage have been represented respectively, as a function of the impact energy. It should be noted that the reported figures only consider impacts in an energy range that does not induce skin failure. As a matter of fact, energies above 200 J resulted in skin failure of the 1 mm skin panels and these results have however not been included in the present research. Nevertheless, in a damage tolerant scenario, for some applications engineers might be more interested on the residual strength of a structure than on the actual

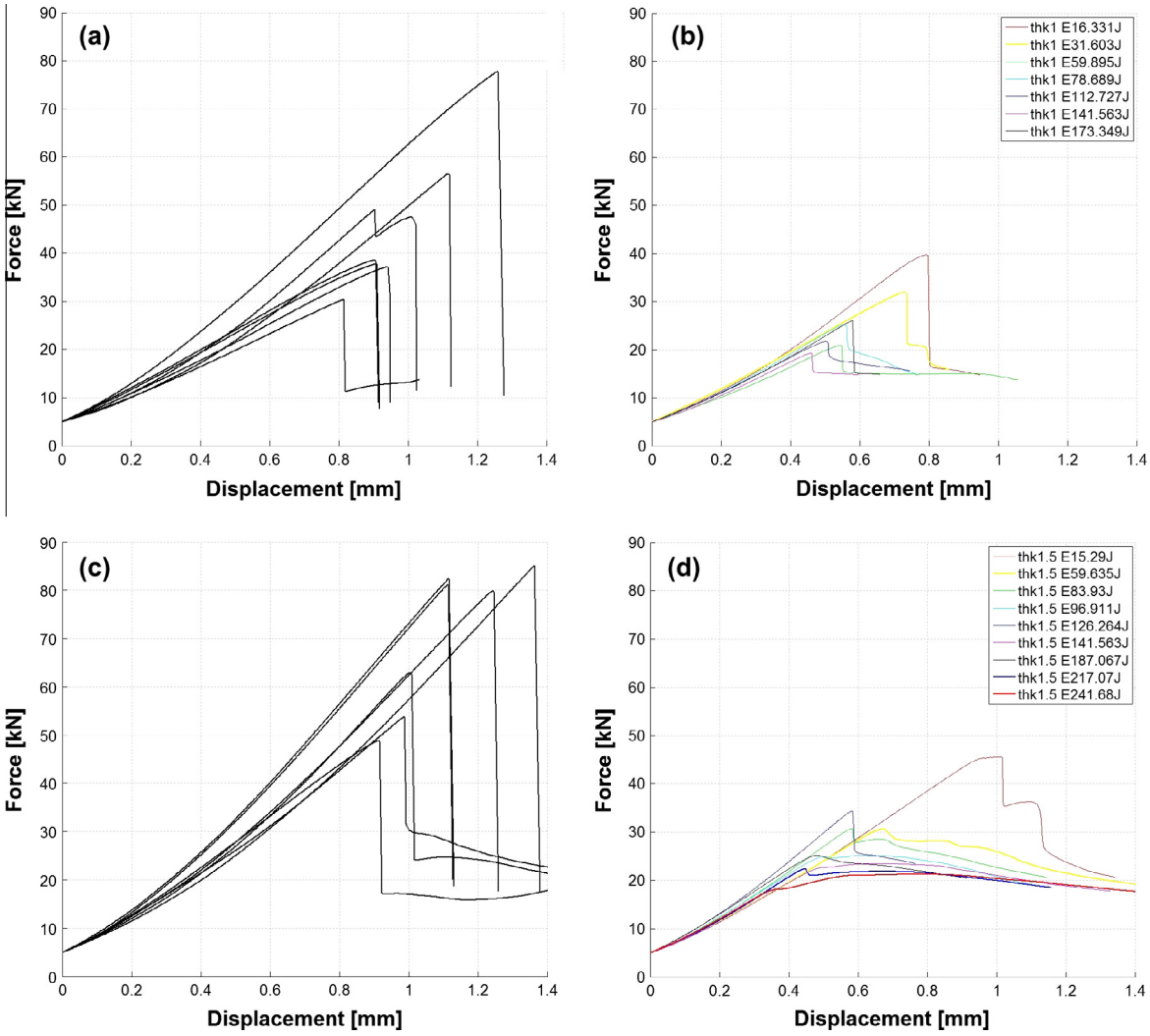

Fig. 6. Experimental compressive force vs. crosshead displacement curves for the CAI and the edgewise compression tests. (a) Intact panels with 1 mm skin thickness, 7 repetitions. (b) Impacted panels with 1 mm skin thickness, 7 repetitions with different impact energies. (c) Intact panels with 1.5 mm skin thickness, 7 repetitions. (d) Impacted panels with 1.5 mm skin thickness, 7 repetitions with different impact energies. The effect of the impact energy on Figures (b), (d) is more clearly shown in Fig. 9c. Curves have been shifted along the horizontal axis in order to reduce the non-linear effect of test rig assembly tolerances.

Table 5
Evaluation of the experimental test variability, comparing the mean (μ) and the standard deviation (σ) of the average stiffness (K) and the deformation energy (U).

	μ_U (J)	σ_U (J)	μ_K (kN/mm)	σ_K (kN/mm)
Thk 1 mm – non impacted	4.57	0.43	41.34	7.92
Thk 1 mm – impacted	4.47	0.24	36.62	3.12
Thk 1.5 mm – non impacted	5.17	0.33	59.13	7.91
Thk 1.5 mm – impacted	4.93	0.28	41.48	3.29

damage (especially if the range of impacts falls below the skin failure threshold, nearly 185 J for the current application and relatively to the 1 mm thick skins). The normalized CAI strength of the considered sandwich panel is reported in Fig. 9c as a function of the impact energy. It has been normalized with respect to the average CAI strength measured for the intact specimens, so that the percentage in the reduction of the performance is more apparent. Indeed Fig. 9c clearly shows that the CAI strength sensitivity to impact energy is particularly high up to a certain threshold (approximately 50 J), above which it remains stable, or at least with a dispensable effect of the impact energy on the CAI strength performances.

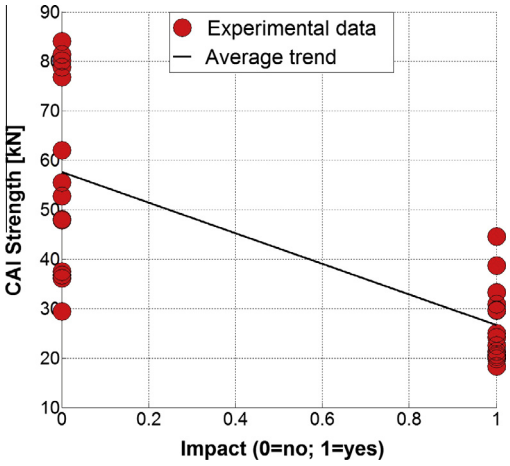

Fig. 7. Effect of the impact condition (undamaged – damaged) on the compression strength of the panels.

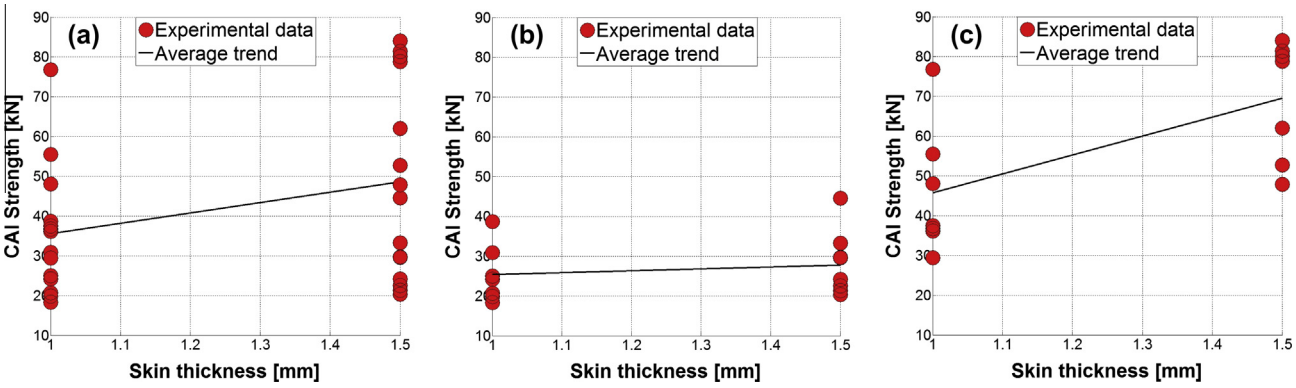

Fig. 8. Effect of the panel skin thickness (1 mm or 1.5 mm) on the compression strength for (a) all the specimens, (b) only impacted specimens and (c) only undamaged specimens.

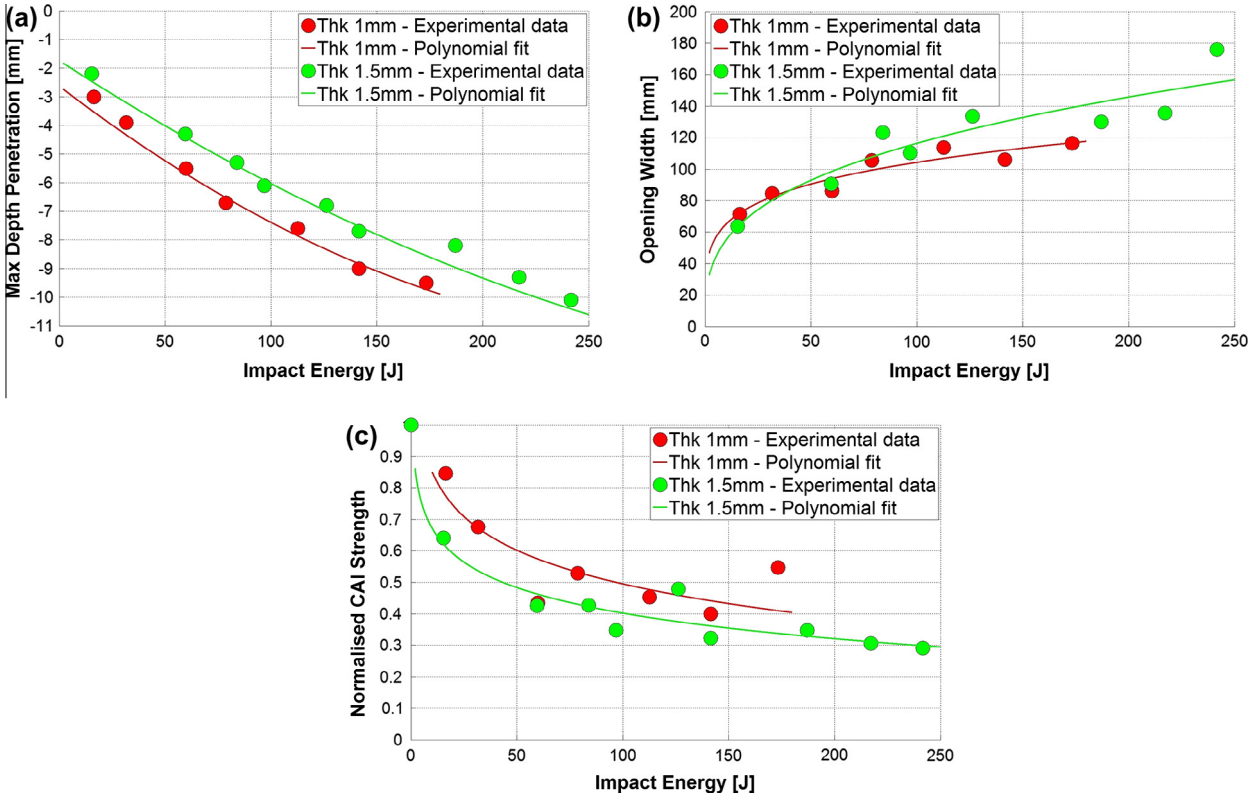

Fig. 9. Effect of the impact energy on (a) the maximum penetration depth, (b) the opening width and (c) the normalized CAI strength.

3.2. Statistical sensitivity analysis

A statistical sensitivity analysis is performed in this section to verify the assumptions made in Section 3.1, based on the interpretation of the graphical data representation. The *analysis of variance* (ANOVA) has been adopted hereafter and MINITAB software has been used to implement it. The application of the ANOVA theory for the current paper is presented in Section 3.2.1. Comments on the obtained results are provided in a separate Section 3.2.2.

3.2.1. Analysis of variance

The *analysis of variance* is a methodology comprehending a series of statistical tools that can be used for many different applications, especially within the design of experiment framework. It provides a quantitative indication of the influence of a set of variables (namely, the factors) over a dependent variable (namely, the observed parameter) and it allows in some cases (when sufficient levels of the factors are taken into consideration) to estimate the parameters of the statistical model that fits the inferred dataset. The ANOVA falls inside the *statistical hypothesis testing* framework and is used here to analyze the means of the observed parameters for different factor configurations in order to decide whether or not they are equal. Suppose a linear statistical model describes the observations from a single factor experiment, like the following:

$$Y_{ij} = \mu + \tau_i + \varepsilon_{ij} \begin{cases} i = 1, & 2, & \ldots, & a \\ j = 1, & 2, & \ldots, & n \end{cases} \tag{3}$$

where Y_{ij} is a random variable indicating the jth observation for the ith level, μ is a parameter common to all the treatments (often referred to as *grand mean*), τ_i is the effect on the observed variable due to a factor at ith level (also referred to as *treatment*), ε_{ij} is a

random error component, a and n are the number of levels and observations per level respectively. In a typical hypothesis testing framework, the ANOVA inference can be based upon the following scheme:

$$H_0 : \tau_1 = \tau_2 = \ldots = \tau_a = 0$$
$$H_1 : \exists i | \tau_i \neq 0 \quad (4)$$

H_0 is the *null hypothesis*, implying that there is no effect of the level chosen for the selected factor, being all the a populations randomly sampled from the same global distribution. If H_0 is not rejected, this will indicate no sufficient evidence against it and the variation of the factor levels appears to have no influence on the observed variable. If H_0 is rejected, it means that there is some evidence of the dependence of the observed variable on the investigated factor levels.

Furthermore, in order to provide a decision based on the ANOVA output, it is necessary to fix the required significance level for the test, or the rate of the *first type error* (α), which is the probability to declare a false dependence on a selected factor, set here to 10%. This parameter has to be chosen as a compromise with the *second type error* (β), which is the probability to un-reject H_0 when some effects of the factor exist. β depends on the significance level (the smaller is α, the bigger β will be), as well as on the sample size and the distance between two population means that wants to be distinguished. The distance is an index of the model sensitivity. The probability to statistically distinguish two population means at a certain distance is an index of test power. Selecting a bigger distance can reduce second type errors but it can at the same time indicate a lower resolution of the statistical model. The solution adopted in this paper is the choice of compromising values summarizing always the β-error for two distance levels of the observed variable (the CAI strength).

The main output of the ANOVA inference is the *P_value*, or the smallest significance level that allows the rejection of the null hypothesis. A small *P_value* indicates large evidence to discard the null hypothesis, thus there is influence of the investigated factor on the observed dependent variable. For each hypothesis test, if the *P_value* is smaller than α, the null hypothesis is discarded and the dependence of the considered factor on the dependent variable is declared.

ANOVA is based on the hypothesis that residuals ε_{ij} are independent and normally distributed with a zero mean and a constant standard deviation. Thus, three conditions have to be verified in order to be able to consider statistically valid the output from the ANOVA inference:

- Independence of the residuals, based here on a graphical verification, however confirmed by the random order in which CAI tests have been performed on different specimens.
- Normality of the residuals, based here on the Anderson–Darling test.
- Homoscedasticity of the residuals (test for equal variances), based here on the Levene test, which is particularly robust for smaller samples, as it is in the current application.

A more detailed explanation of the tests for the residual analysis is beyond the scope of the present paper and the interested reader can refer to [24], [25] for a deeper insight into the ANOVA method. The only necessary information is that a positive outcome from the tests requires the associated *P_value* to be above a predefined significance level (α is set to 5% for the residual tests). In case one or more of the requirements are not met, one can resort to data transformation; in particular, the *Box–Cox* transformation has been successfully adopted in the current framework, when necessary.

The authors remark that the experimental program herein described considers one observed variable (compressive strength) and three factors (impact occurrence, impact energy and thickness). ANOVA can be used to contemporaneously test the influence of many factors on an observed variable. In a multi-factor framework, it is possible to study the influence of factor interaction (higher order factors). For the purposes of the current activities, a preliminary application of a two-ways ANOVA evidenced the non-influence of higher order factor interactions and only the first order factors are therefore be considered hereafter. Some of the tests reported hereafter (when only two factor levels have been observed) could have been performed with a *t-test* [25]. When applicable, both methods have been implemented and result consistency between ANOVA and *t-test* has been verified. However, in order to provide a homogeneous description, only the ANOVA results have been reported hereafter.

Following the factor scheme investigated in Section 3.1, three main tests have been performed:

- Impact (damaged/undamaged) influence on the compressive strength of a sandwich panel.
- Skin thickness influence on the compressive strength of a sandwich panel.
- Impact energy influence on the CAI strength of a sandwich panel.

It is however important to underline that, while some test repetitions have been considered concerning the impact condition and the skin thickness factors, only one test has been executed at each level of the impact energy.

In order to apply the ANOVA methodology to evaluate the influence of the impact energy, data have been grouped into bins according to the impact energy range they belong to (Fig. 10a). In particular, three groups have been established, as reported in Table 6 (Energy – Case 1), namely [0–50 J], [50–130 J] and [130–250 J] and the influence of the impact energy on the CAI strength has been evaluated, including only the impacted specimens into the inference process. Another test has been executed comparing only those impact cases falling into the second and third group (Energy – Case 2).

All the results of the statistical inference problem have been summarized in Tables 6–8 and are commented on in detail in the following Section. In particular, the ANOVA results are presented in Table 6 while the positive outcomes from the ANOVA validation tests on the residuals are shown in Table 7. Finally, having fixed the first type error deliberately to 10%, an estimation of the second type error is provided in Table 8 for each inference test.

3.2.2. Analysis of the results

The first analyzed case is the influence of the impact on the compressive strength of the sandwich panel, as previously assessed in Fig. 7. Impacted specimens have been compared with intact specimens to highlight any systematic reduction of the CAI strength due to impact. The obtained *P_value* is clearly below the 10% α-threshold defined above, demonstrating the dependence of the CAI strength on the occurrence of the impact damage. The test power (and consequently the second type error) has been reported in Table 8. It has been calculated assuming an average sample size of 15 and a standard deviation of 13.3 kN, based on the data reported in Table 4. According to the specific dataset, the probability to miss a 10 kN reduction of the CAI strength is 35.8%, while it reduces to 0.9% if a 20 kN reduction is considered. Nevertheless, as clearly visible in Fig. 7, the average CAI strength reduction is much higher than 20 kN and indication of impact influence on compressive strength was found.

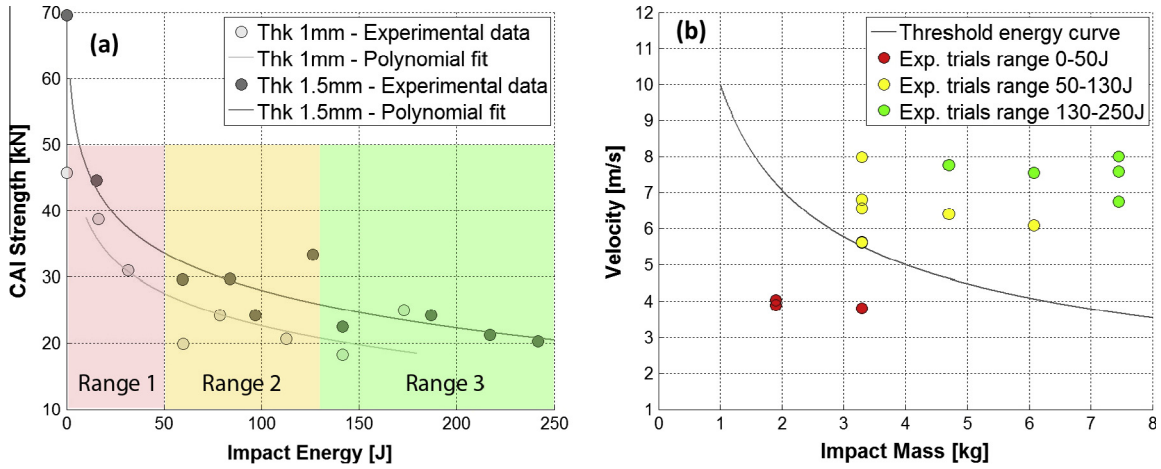

Fig. 10. (a) CAI strength as a function of impact energy; the allocation of the data to three energy ranges in order to apply ANOVA is highlighted (b) threshold velocity-mass curve relative to 50 J impact and different velocity-mass combinations adopted during experiments. The figure allows appreciating the energy threshold in terms of more physical parameters (impactor mass and velocity).

Table 6
Summary of the ANOVA results; the influence of a factor on the CAI strength is declared comparing the *P*-value with a significance level.

Inference	Database	*P_value*	Influence criterion	Influence on CAI strength
Impact occurrence	All	0.000	*P_value* < 0.1	Yes
Skin thickness (Case 1)	All	0.282	*P_value* < 0.1	No
Skin thickness (Case 2)	Impacted specimens	0.472	*P_value* < 0.1	No
Skin thickness (Case 3)	Undamaged specimens	0.015	*P_value* < 0.1	Yes
Impact energy (Case 1)	Impacted specimens [0–50 J] vs. [50–130 J] vs. [130–250 J]	0.001	*P_value* < 0.1	Yes
Impact energy (Case 2)	Impacted specimens [50–130 J] vs. [130–250 J]	0.105	*P_value* < 0.1	No

Table 7
Summary of results for the ANOVA test validation; independence, normality and homoscedasticity of residuals are the three hypothesis to be verified in order to be able to consider the ANOVA results statistically valid.

Inference	Normality of residuals (Anderson–Darling test)	Independence of residuals	Homoscedasticity of residuals (Levene test)
Impact occurrence	Yes (*P_value* = 0.403)	Yes	Yes (*P_value* = 0.755)
Skin thickness (Case 1)	Yes (*P_value* = 0.149)	Yes	Yes (*P_value* = 0.205)
Skin thickness (Case 2)	Yes (*P_value* = 0.729)	Yes	Yes (*P_value* = 0.851)
Skin thickness (Case 3)	Yes (*P_value* = 0.836)	Yes	Yes (*P_value* = 0.923)
Impact energy (Case 1)	Yes (*P_value* = 0.926)	Yes	Yes (*P_value* = 0.341)
Impact energy (Case 2)	Yes (*P_value* = 0.836)	Yes	Yes (*P_value* = 0.180)

Table 8
Evaluation of the test power and the second type error for all the tests.

Inference	Sample size	Estimated standard deviation (kN)	Required distance (kN)	First type error (%)	Test power (%)	Second type error (%)
Impact occurrence	15	13.3	10	10.0	64.2	35.8
			20	10.0	99.1	0.9
Skin thickness (Case 1)	15	11.5	10	10.0	38.0	62.0
			20	10.0	84.0	16.0
Skin thickness (Case 2)	8	7.4	10	10.0	82.2	17.8
			20	10.0	99.9	0.1
Skin thickness (Case 3)	7	15.6	10	10.0	30.6	69.4
			20	10.0	73.1	26.9
Impact energy (Case 1 and 2)	6	7.3	10	10.0	71.3	28.7
			20	10.0	99.7	0.3

The focus is now transferred onto the skin thickness influence on the panel compressive strength. If the overall data are considered (impacted and intact specimens), and if a maximum 10% first type error rate is admitted, thickness has no influence on the compressive strength. Nevertheless, given the average sample size (15 samples), the estimated standard deviation (11.5 kN) and the selected first type error rate (10%), the probability to miss even a 20 kN reduction of the compressive strength has been quantified as 16.0%. As depicted also in Fig. 8, a net increase of the inference precision can be obtained considering impacted and intact specimens separately. ANOVA declares that skin thickness has no influence on the CAI strength for the impacted specimens while

it does have an effect on compressive strength for the intact, undamaged, specimens. Nevertheless, it is important to consider the probability of the second type error, especially when the null hypothesis is not rejected (as happens for the impacted panels). In practice, the acceptance of the ANOVA output strongly depends on what the designers intend as a valid engineering sensitivity. Based on the results reported in Table 8, the probability to have missed a 10 kN variation of the CAI strength is 17.8%, while it is reduced to 0.1% if a 20 kN variation is considered. If a 20 kN variation is considered as a minimum reasonable threshold for engineering sensitivity, one can assume that no effect of skin thickness over the CAI strength is statistically evident from the available database, with reasonable confidence (second type error rate of 0.1%). The smaller the average shift one is interested to recognize, the lower is the confidence in the ANOVA output. As a conclusion, skin thickness has an effect on compressive strength, which is sensibly reduced when the impact damage occurs on the panel skin. As a matter of fact, the flexural stiffness of the panel increases if a thicker skin is adopted. Nevertheless, the presence of an impact damage induces an asymmetry on the panel which facilitates bucking, thus reducing the benefits of a more rigid skin. The authors intend to remark that, within the impacted specimens, CAI strength was measured in correspondence of different impact energies. This would not be the best scenario for the evaluation of skin thickness influence, nevertheless it is worth to remind to the reader that approximately the same energy ranges were adopted while testing the two levels of skin thickness thus allowing reasonable comparisons.

Finally, the influence of the impact energy over the CAI strength of sandwich panels is analyzed. Referring to Fig. 9c, it has been anticipated that the impact energy influences the CAI strength, nevertheless this influence remains almost constant above a certain threshold (about 50 J). For this reason, data have been grouped firstly in three ranges (Case 1), namely [0–50 J], [50–130 J] and [130–250 J], as shown in Fig. 10a. ANOVA indicates dependence of the CAI strength on the impact energy. Nevertheless, when only the second and third ranges are compared (Case 2) no sufficient evidence is present on the available data to reject the null hypothesis, thus no influence of the impact energy on the CAI strength is declared for impact energies above 50 J. Again, it is important to check the test power and the second type error rate. Six samples are present on average in each range and a standard deviation of 7.3 kN has been estimated based on the data presented in Table 4 (considering only the impacted specimens). Given a 10% first type error rate is fixed, the probability to miss a 10 kN reduction of the CAI strength is 28.7%, while it reduces to 0.3% if a 20 kN reduction is considered. As a conclusion, the CAI strength decreases while the impact energy increases; nevertheless, this is valid up to a certain threshold (50 J), above which a reduced influence of the impact energy on the CAI strength has been evidenced. However, it should be taken into consideration that there is 28.7% probability that the CAI strength reduces by 10kN in the [50–250 J] range. Furthermore, referring to Fig. 9c, the influence of the skin thickness on the identified impact energy threshold appears to be minimal, in agreement with the results obtained while investigating skin thickness influence over the impacted specimens. What is interesting is that even though the threshold can be considered the same for both thickness configurations, the normalized CAI strength shows a higher decrement for the 1.5 mm skin thickness compared with the 1 mm one. The reason is that after the threshold, the CAI strength is very similar for both panel configurations but regarding the intact condition, the 1.5 mm ones have obviously a higher CAI strength. The consequence is that the normalization leads to a lower curve for the 1.5 mm skin thickness compared with the 1 mm thickness (Fig. 9c). This shows how the relative decrement of performance is higher for the thicker skins panels compared with the thinner ones.

The threshold curve corresponding to 50 J has been plotted in Fig. 10b, in terms of mass and velocity that provide 50 J kinetic energy. The threshold curve is built on the simple calculation of the kinetic energy whilst each experimental point is placed on the graph, being the impactor mass and velocity known for each experimental test. Fig. 10b allows quantifying in a more physical way the impact condition above which the CAI strength is minimally influenced by impact energy.

4. Conclusions

Sandwich panels with thin aluminum skins and a Nomex™ honeycomb core are attractive as they can considerably reduce the weight while maintaining very good mechanical properties. The use of aluminum alloy for the skins, a ductile material able to absorb energy by localized deformation, makes such panels an interesting option when low velocity impacts are an unavoidable threat. However, the residual strength of such structures (in terms of compressive loads) when subjected to impact damage is poorly studied in the literature exactly when metallic skins are used (commonly only full composite sandwich panel have been mainly investigated up to the present time). A test program based on compression after impact tests has been carried on and results have been reported, and statistically interpreted in the present paper through the well-known analysis of the variance (ANOVA) methodology.

CAI or edgewise compression strengths are relative to the peak load that is obtained in the force–displacement curve during tests. If the entire force–displacement curve is considered, some additional information can be retrieved. In particular, while the occurrence of an impact does not change the expected values of the structural stiffness and the deformation energy, it has a marked effect on the standard deviation of these two parameters. In particular, referring to the tests executed in the framework of this study, curves associated to intact specimens have a standard deviation, which is double compared with the same curves calculated on impacted specimens. This is assumed to be related to the honeycomb contribute to bucking resistance, coupled to the geometrical cell structure: once the core is damaged, its ability to carry the load becomes negligible so the buckling load depends only on skins, which are much more homogeneous than the core. In case of intact panel, edgewise strength depends both on core and skin but honeycomb is everything but homogeneous thus this leads to a relevant dispersion of the force–displacement curves.

The residual compressive strength after impact damage (CAI strength) has been compared with the initial compressive strength (edgewise compression strength) and a significant influence of the impact damage has been found.

The contribution of the skin thickness to the compressive load resistance has been addressed. In practice, increasing the skin thickness can produce a stiffer structure with more bending resistance, resulting in a higher compressive strength (for the undamaged panel). Nevertheless, if impact damage occurs, the benefits related to the adoption of a thicker skin are strongly reduced, especially if the drawbacks due to the additional weight are taken into consideration. However, it is worth to mention that skin thickness is particularly important when the breakage of skins is concerned. Using a thicker specimen, higher impact energy can be reached without skin fracture [2]; although skin failure has not been considered in the present article the latter consideration may be useful for design purpose. However, for common applications, and especially in the SHM framework, skin fracture is considered just an extreme scenario. Of much higher interest is the energy range that generates plastic deformation damage but not fracture. Quantitatively an increment of skin thickness from 1 to 1.5 mm leads to

an increment of the overall panel weight of 44% and the corresponding edgewise strength experimentally increases of 36%. Once the panel has been damaged, there is no statistical evidence of the skin thickness effect on the CAI strength. Hence, from a design point of view, it is worth incrementing the skin thickness if panels are going to be deployed in an environment where there is almost no possibility of a low velocity impact. Instead, in scenarios where low velocity impacts are probable, it is not worth incrementing the skin thickness with the aim to increase residual strength because its effect on CAI strength (vs. mass increment) of the impacted structure is reduced.

Concerning impact energy, the impact damage increases as a function of the energy associated to the impact. Nevertheless, the CAI strength significantly reduces as a function of the impact energy only up to a certain energy threshold (set here to 50 J). No evidence of a CAI strength reduction has been found for higher impact energies, though they were obviously associated to bigger damages [2]. Nevertheless, only impacts involving no skin failure (through crack) have been included into the current analysis (the maximum impact energy that has been considered was 173 J and 241 J for the 1 mm and 1.5 mm thick skin respectively).

This result might be particularly advantageous in the perspective of the realization of SHM systems for impact monitoring. As a matter of fact, given that a sensor network is deployed on the structure and a signal processing methodology is able to correctly estimate the position and the energy of the impact, it is possible to correlate the impact characteristics with the residual structural strength, which is one of the major requirements in a damage tolerant scenario. Furthermore, depending on the use case scenario, if impacts are expected to be above a certain threshold, the design of SHM systems for energy quantification can be avoided, focusing the attention on the impact detection and localization performances only.

Acknowledgements

This work has been developed and is based on the project "STIMA – Strutture Ibride per Meccanica ed Aerospazio", a research project co-funded by the Regione Lombardia in the framework of the R&D call for "energy, environment, agro-food systems, health and advanced manufacturing".

References

[1] Aminanda Y, Castanié B, Barrau JJ, Thevenet P. Experimental analysis and modeling of the crushing of honeycomb cores. Appl Compos Mater 2005;12:213–27.
[2] Manes A, Gilioli A, Sbarufatti C, Giglio M. Experimental and numerical investigations of low velocity impact on sandwich panels. Compos Struct 2013;99:8–18.
[3] C 364/C 364M – 07. Standard test method for edgewise compressive strength of sandwich constructions.
[4] Standard Tests for Toughened Resin Composites. NASA reference publication 1092, ACEE composites project office, Langley research center (Hampton, Va.), 1982.
[5] Advanced Composite Compression Tests. Boeing specification support standard BSS 7260, Rev. C, The Boeing Co. (Seattle, Wash.), December 1988.
[6] ASTM D 7136. Test method for measuring the damage resistance of a fiber-reinforced polymer matrix composite to a drop-weight impact event. ASTM International, W. Conshohocken, Pa., 2005.
[7] ASTM D 7137. Test method for compressive residual strength properties of damaged polymer matrix composite plates. ASTM International, W. Conshohocken, Pa., 2005.
[8] Tomblin J, Lacy T, Smith B, Hooper S, Vizzini A, Lee S. Review of damage tolerance for composite sandwich airframe structures. FAA William J. Hughes Technical Center, Atlantic City International Airport, New Jersey, DOT/FAA/AR-99/49, August 1999.
[9] Tomblin JS, Raju KS, Liew J, Smith BL. Impact damage characterization and damage tolerance of composite sandwich airframe structures. FAA William J. Hughes Technical Center, Atlantic City International Airport, New Jersey, DOT/FAA/AR-00/44, January 2001.
[10] Aminanda Y, Castanié B, Barrau JJ, Thevenet P. Experimental and numerical study of compression after impact of sandwich structures with metallic skins. Compos Sci 2009;69:50–9.
[11] Lacy TE, Hwang Y. Numerical modeling of impact-damaged sandwich composites subjected to compression-after-impact loading. Compos Struct 2003;61:115–28.
[12] Gustin J, Joneson A, Mahinfalah M, Stone J. Low velocity impact of combination Kevlar/carbon fiber sandwich composites. Compos Struct 2005;69:396–406.
[13] Schubel PM, Luo JJ, Daniel IM. Impact and post impact behavior of composite sandwich panels. Compos Part A: Appl Sci 2007;38:1051–7.
[14] Shipsha A, Zenkert D. Compression-after-impact strength of sandwich panels with core crushing. Appl Compos Mater 2005;12:149–64.
[15] Harvey R, Kemp M, Wolf K. A compression test method for damaged fibre reinforced plastic sandwich specimens. In: Allen HG, editor. Sandwich construction 3, vol. II. Cradley Heath, UK: EMAS Publishing; 1996. p. 669–76.
[16] Klaus M, Reimerdes HG, Gupta NK. Experimental and numerical investigations of residual strength after impact of sandwich panels. Int J Impact Eng 2012;44:50–8.
[17] Meng L, Chen S, Wu Y, Shu X. Projectile impact behaviour of sandwich material with Nomex honeycomb and metallic skins. Adv Mater Res 2011;204–210:632–5.
[18] Giglio M, Gilioli A, Manes A. Numerical simulation of ballistic impact on sandwich panels with Nomex™ honeycomb core. In: Proceedings of the 3rd international conference on composite structures ICILLS 2011, Valenciennes, France, June 28th–July 1st, 2011.
[19] Giglio M, Manes A, Gilioli A. Investigations on sandwich core properties through an experimental–numerical approach. Compos Part B-Eng 2012;43:361–74.
[20] Giglio M, Gilioli A, Manes A. Numerical investigation of a three point bending test on sandwich panels with aluminum skins and Nomex™ honeycomb core. Comput Mater Sci 2012;56:69–78.
[21] Giglio M, Gilioli A, Sbarufatti C, Manes A. SHM application on sandwich panels with Nomex™ honeycomb core and aluminium skins subjected to low velocity impacts. In: Proceedings of the 15th European conference on composite materials, Venice – Italy 24–28 June 2012.
[22] Frieden J, Cugnoni J, Botsis J, Gmur T. Low velocity impact damage monitoring of composites using dynamic strain signals from FBG sensors – Part I: Impact detection and localization. Compos Struct 2012;94:438–45.
[23] Hexcell Corporation. HexWeb® HRH-10, Aramid fibre/phenolic honeycomb, Product data.
[24] Montgomery DC. Design and analysis of experiments. 5th ed. New York: John Wiley & Sons; 2001.
[25] Montgomery DC, Runger GC. Applied statistics and probability for engineers. New York: John Wiley & Sons; 2003.